Lunar Iron and Uranium Distribution Obtained by SELENE(Kaguya) Gamma-ray Spectrometer. M. Hareyama[1], Y. Karouji[1], N. Yamashita[4], Y. Fujibayashi[2], H. Nagaoka[2], N. Hasebe[2], S. Kobayashi[3], R.C. Reedy[4], C. d'Uston[5], O. Gasnault[5], O. Forni[5], K. J. Kim[6] and the Kaguya Gamma Ray Spectrometer team. [1]Japan Aerospace Exploration Agency, Kanagawa, Japan (hareyama.makoto@jaxa.jp), [2]Res. Inst. for Sci. & Eng., Waseda University, Tokyo, Japan, [3]National Institute of Radiological Sciences, Chiba, Japan, [4]Planetary Science Institute, Tucson, AZ, USA, [5]Institut de Recherché en Astrophysique et Planétologie, Université de Toulouse, CNRS, Toulouse, France, [6]Korea Institute of Geosciences & Mineral Resources, Dajeon, South Korea.

Introduction: The Kaguya(SELENE) gamma ray spectrometer (hereafter KGRS) [1] has observed lunar gamma rays to determine elementary distributions on lunar surface. The KGRS was in orbit about an average altitude of 100km from Dec. 2007 to Dec. 2008, and then it was changed to an average altitude of 50 km from Jan. 2009 to May 2009. The KGRS employed a high-purity germanium crystal for main detector and plastic and bismuth germanate (BGO) scintillators for anti-coincidence detectors to reduce background noise from charged particles. When counts occurred simultaneously in the Ge and BGO detectors, the Ge signal was ignored.

Up to now, natural radioactive elements such as potassium, thorium and uranium are reported by using the data obtained at 100 km altitude [2,3]. For the heavy major elements, calcium has been mapped by using the data at 50 km altitude [4]. This work reports the maps of lunar iron and uranium and their correlation based on the data measured in 50 km altitude.

The lunar gamma rays except for natural radioactive elements should be corrected neutron density because of their emission by the interaction of neutrons with lunar nuclei. As mentioned in Ref. [4], since variations of observed neutron-capture gamma rays for some elements are greatly dominated by the fluxes of thermal neutrons, elemental analysis on the basis of inelastic scattering gamma rays has the clear advantage of low dependency on neutron variations. Therefore, this work derives the iron distribution from an inelastic-scattering gamma ray.

Data Processing and Analysis: Gamma-ray counts obtained by the KGRS at lower altitude were accumulated using the moving-average technique, i.e., every 2 deg. in longitude and latitude with the radius of 150 km. Net counting rates of gamma rays were determined by peak fitting for a better understanding of the complicated spectra [5].

To derive elemental distribution of iron and uranium, two gamma ray peaks were selected. One is 609 keV peak for uranium and the other is 846 keV peak for iron that made from inelastic scattering process as ^{56}Fe(n,nγ) reaction. Both peaks exist on irregular shape peaks called sawtooth peaks [6]. This peak is produced by Ge(n,nγ) reaction that is inelastic scattering of a lunar fast neutron inside the HPGe detector and detected by the detector itself. Therefore, it was difficult to fit such peaks on the sawtooth peak recognized as interference peak, although each 609 keV for U and 846 keV for iron is the largest gamma ray peak for each element in lunar gamma ray energy spectrum from 200 keV to 12 MeV. However, since we have developed the fitting method for sawtooth peak as shown in Fig. 1 as an example [7], it is possible to make a reliably estimate for these peak intensities as well as that for sawtooth peak. After deriving net counting rates, altitude and neutron corrections were applied with using fast neutron data derived from sawtooth fitting.

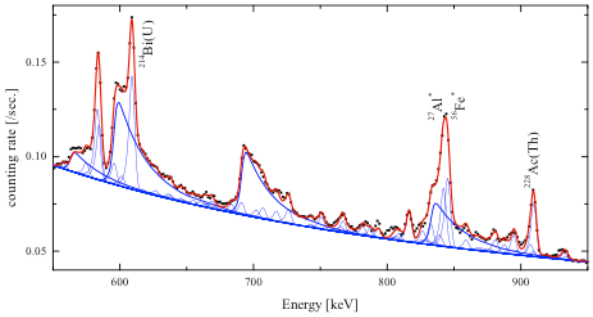

Fig. 1. An example of peak fitting with 'sawtooth' peaks. Some big peaks are on a wide 'sawtooth' feature (blue thick lines) at 609 keV from U, 844 keV from Al and 847 keV from Fe.

Results: The maps for uranium and iron are shown in Fig. 2 and Fig. 3. Both maps are translated to concentration from net counting rate after the corrections by ground truth method using Apollo and Luna returned samples [8].

The uranium distribution obtained by this work was compared with the other independent result obtained from the data in 100 km altitude [3], which was estimated the uranium abundance by analytical calculation method [2]. The results of absolute value are in good agreement with each other. This fact may indicate that our ground truth method gives a reliable estimation.

The iron oxide map of absolute concentration gives almost similar distribution to the Lunar Prospector GRS result [9]. Basically, iron abundance is high in

mare region and low in highland region. The highest region is in Oceanus Procellarum.

Based on compositions of lunar thorium and iron in lunar materials such as lunar meteorites and Apollo returned samples, lunar rocks can be classified as three main types [e.g. 10]. First is a feldspathic material (highland), second is a basaltic composition (maria) and third is a KREEP material. In Fig. 4, the correlation between uranium and iron oxide is presented instead of lunar thorium. In the Moon, thorium and uranium has similar geochemical behavior. The result indicates high iron and high uranium abundances out of a triangle correlation given by lunar materials, where those compositions are not found in lunar materials. These compositions are found in Oceanus Procellarum and Mare Imbrium. The similar result has been already reported in the correlation between iron and thorium observed by LPGRS [9] .

Summary: In this work, global maps of lunar uranium and iron oxide and their correlation are reported on the basis the low altitude data at 50 km obtained by Kaguya GRS observation. The results are consistent with the past results.

References: [1] Hasebe, N. et al., (2008) *Earth, Planets, and Space*, 60, 299-312. [2] Kobayashi, S. et al., (2010) *Space Sci. Rev.*, 154, 193-218. [3] Yamashita, N. et al., (2010) *Geophys. Res. Lett.* 37, L10201. [4] Yamashita, N. et al., (2012) *Earth Planet. Sci. Lett.* 353-354, 93-98. [5] Yamashita, N. et al., (2012) *43rd LPS* Abstract #1283. [6] Brückner J. et al. (1987) Proc. Lunar Planet. Sci. Conf. 17th, *JGR* 92, E603. [7] Hareyama, M. et al., (2011) *42nd LPS* Acstract #1687. [8] Lucey, P., et al., (2006) *Rev. Mineral. Geochem.* 60, 83. [9] Prettyman T. H. et al. (2006) *JGR* 111, E12007. [10] Jollif. B.L. at al., (2000) *JGR* 105, 4197. [11] Data compiled in Lunar Meteorite Compendium at NASA Astromaterials Acquisition and Curation Office. http://curator.jsc.nasa.gov/antmet/lmc/lmc_cc.cfm

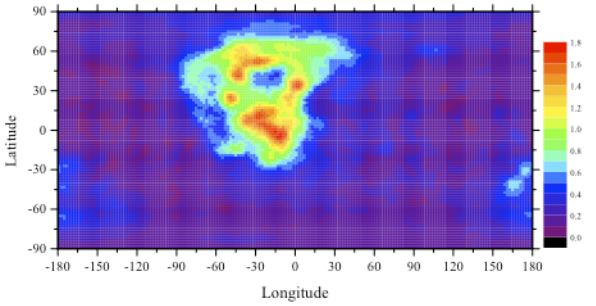

Fig. 2 The uranium abundance map. Gamma ray counts accumulated from the radius of 150 km with every 2 degrees grid in the data collected at 50 km altitude. Color bar indicates uranium concentration in ppm.

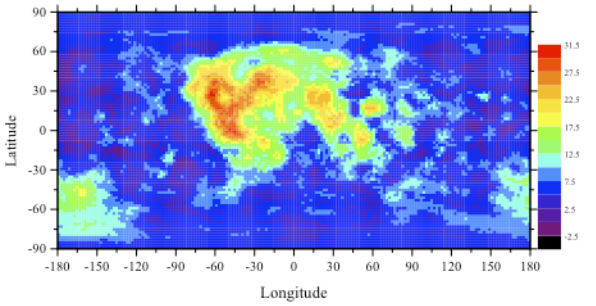

Fig. 3 The iron oxide abundance map. Gamma ray counts accumulated from the radius of 150 km with every 2 degrees grid in the data collected at 50 km altitude. Color bar indicates the concentration in wt%.

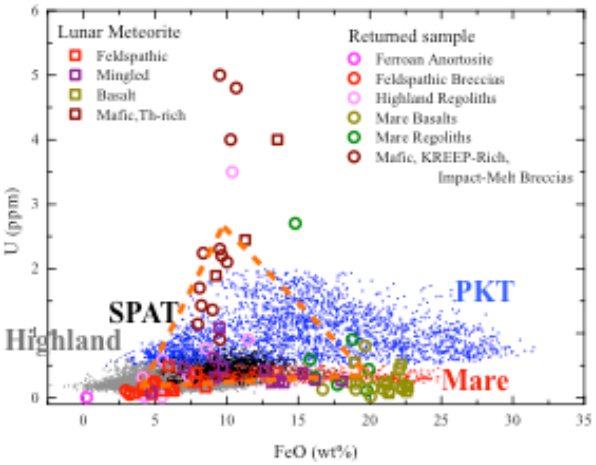

Fig. 4 The correlation of abundance between iron and uranium. Circles remark Apollo samples [8] and squares remark lunar meteorites [11]. Dots indicate KGRS result; blue dots are Procellarum KREEP Terrain (PKT), red dots are Mare Region except for Oceanus Procellarum and Mare Imbrium in PKT, black dots are South Pole Aitken Terrain (SPAT) and gray dots are highland. each vertex of a triangle indicates an average value of each type of lunar materials.